

Global Assessment of PA variability through concurrent Physics-based X-parameter and Electro-Magnetic simulations

*Original*

Global Assessment of PA variability through concurrent Physics-based X-parameter and Electro-Magnetic simulations / Donati Guerrieri, S.; Ramella, C.; Bonani, F.; Ghione, G.. - ELETTRONICO. - (2021), pp. 213-216. (Intervento presentato al convegno 15th European Microwave Integrated Circuits Conference, EuMIC 2020 tenutosi a Utrecht, Netherlands nel 10-15 January 2021) [10.1109/EuMIC48047.2021.00065].

*Availability:*

This version is available at: 11583/2872834 since: 2021-03-01T16:24:06Z

*Publisher:*

Institute of Electrical and Electronics Engineers Inc.

*Published*

DOI:10.1109/EuMIC48047.2021.00065

*Terms of use:*

This article is made available under terms and conditions as specified in the corresponding bibliographic description in the repository

*Publisher copyright*

IEEE postprint/Author's Accepted Manuscript

©2021 IEEE. Personal use of this material is permitted. Permission from IEEE must be obtained for all other uses, in any current or future media, including reprinting/republishing this material for advertising or promotional purposes, creating new collecting works, for resale or lists, or reuse of any copyrighted component of this work in other works.

(Article begins on next page)

# Global Assessment of PA variability through concurrent Physics-based X-parameter and Electro-Magnetic simulations

S. Donati Guerrieri<sup>1</sup>, C. Ramella<sup>1</sup>, F. Bonani<sup>1</sup>, G. Ghione<sup>1</sup>

<sup>1</sup>Dipartimento di Elettronica e Telecomunicazioni, Politecnico di Torino  
Corso Duca degli Abruzzi, 24, I-10129 Torino, ITALY

**Abstract**— The novel technique introduced in [1] is exploited to address a full variability analysis of a GaAs MMIC X-band power amplifier, including the statistical variations of several technological parameters, both in the active and passive components. The active device is modelled by means of X-parameters, directly extracted from physics-based analysis. A non-50  $\Omega$  X-Par model is used to take into account the input port mismatch with respect to the conventional 50  $\Omega$  reference. The scattering parameters of the passive structures are extracted from accurate electromagnetic simulations and then imported into the circuit simulator through data interchange files (e.g. MDIF or CITIfile) as a function of the most important MMIC fabrication parameters, e.g. the thickness of the MIM capacitor dielectric layer. The analysis shows that more than 10% of output power variations can be ascribed to the concurrent MIM and doping variations in conventional GaAs MMIC technology.

**Keywords**— Device variability, microwave amplifiers, X parameters

## I. INTRODUCTION

The design of nonlinear microwave circuits critically relies on the dependability of the model used for both the active device and passive structures. Unfortunately, the fabrication of nonlinear circuits, both at MMIC and hybrid level, is affected by fabrication tolerances, which ultimately make the overall circuit performance severely dependent on process variability. Such variations can be accounted for only when a direct link between the adopted models and the underlying physical parameters is retained, a link in most cases lost in nonlinear active device models. For passive structures, technological variations can be in principle accounted for by electromagnetic (EM) analysis, albeit at the cost of computationally intensive simulations, especially when full 3D EM models are used. As a result, reliable and computationally efficient variability analysis of a nonlinear stage, including statistical analysis with several concurrent, and possibly correlated, parameter variations is not readily available within conventional design strategies.

In this paper, we exploit a recently proposed method [1] to demonstrate the global statistical analysis of a nonlinear stage, namely an MMIC X-band power amplifier (PA), including the spread of technological parameters affecting both the active device and the passive semi-distributed structures. The analysis is completely carried out within a CAD framework (here Keysight ADS [2]), allowing for very fast and numerically

efficient statistical simulations. Active devices are modelled at circuit level through X-parameters (X-par) [3], while passives are described by parametrized S-parameter files (MDIF/CITIfile). In [1] the PA design and statistical analysis was limited to the output matching network, whereas in this paper it is extended to the full power stage, including the input matching network. This requires the X-par model to be modified, to take into account the high input port mismatch with respect to the standard 50  $\Omega$  environment.

## II. MULTIPHYSIC MODELING OF NONLINEAR STAGE VARIABILITY

Fig. 1 shows the scheme of the proposed methodology. The active device is connected to external passive structures (including the bias network) by means of interconnection ports. Both the active and passive structures are subject to statistical technological variations, e.g. varying doping concentrations, gate workfunction, polarization charge or dielectric layers thickness. All such variations can be accounted for by physics-based analysis, namely physics-based (e.g. drift-diffusion) nonlinear Technology CAD (TCAD) simulations [4], [5], [6] for the active device, and EM simulations for the passive structures. For nonlinear circuits, TCAD and EM simulations cannot be carried out independently, since the passive structure variations also impact the device Large Signal Operating Point (LSOP): as such, this is a typical example of multi-physics problem. Physics-based statistical simulations, though, are extremely time-consuming and not prone to circuit design. Furthermore, while EM tools are directly accessible or linked within standard RF/microwave EDA tools, the same is not the case for TCAD. To overcome these limitations, in [1] physical simulations are used as the starting point to extract circuit level models, yet capable to retain, with high accuracy, the dependency to selected technology parameters, i.e. *parametrized circuit models*.

The most effective way to build-up a parametrized model is through a look-up table, where data are interpolated as a function of the selected parameters.

For active devices, X-pars are the ideal nonlinear model to directly import the results from physics based analysis into circuit-level simulations, exploiting the link with the device Conversion Matrix [7]. Multiple physical simulations

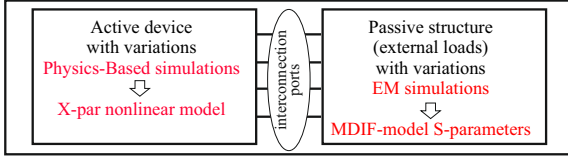


Fig. 1. Multiphysics variability analysis of a nonlinear stages [1].

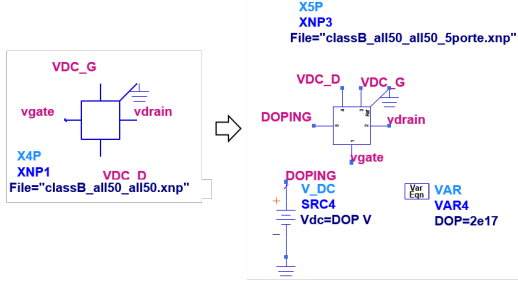


Fig. 2. X-par with extra port DOPING used for interpolation over physical parameters in the X-par file.

with varying technological parameters, readily allow for a *parametrized X-par model*. As an example, Fig. 2 shows an FET X-par model, including two DC and two RF ports. To make the model dependent, e.g., on doping, an extra, fictitious, DC port is added, isolated from all others, allowing to interpolate data in the X-par file as a function of the doping concentration. Multiple parameters can also be accounted for by means of multi-dimensional interpolation.

Passive structures can be represented by conventional S-parameters as a function of frequency, e.g. the fundamental and its harmonics, and of any other relevant technological parameter. EM simulations are used to extract parametrized S-parameters, then stored in a data interchange file. Fig. 3 shows an example of a two-port CITIfile, containing the S-parameters of a PA output matching network as a function of the thickness of the SiN layer used for MIM capacitors, up to the 5-th harmonic.

Finally, once the parametrized models are defined, statistical analysis of a full nonlinear stage is readily viable at circuit level through the standard MonteCarlo analysis implemented in microwave simulators [8], [9], see e.g. Fig. 4. Notice that variations of the passive networks can be viewed as load variations at the device output port, i.e. a particular case of load-pull around the design optimum impedance. From the simulation standpoint, this is equivalent to a synthesized load-pull analysis where the harmonic loads are independently varied: a kind of analysis for which X-pars are extremely well suited, since they represent a local device model around a nominal LSOP.

### III. ACTIVE DEVICE X-PAR MODEL

In this work we address the statistical analysis of a deep class AB tuned load PA (10%  $I_{DSS}$ ) at 12 GHz. Previous

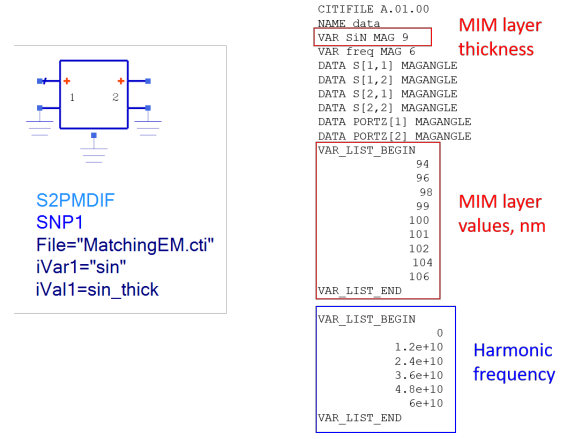


Fig. 3. S2PMDIF component used for passive structures as a function of a technological parameter, here the thickness of the SiN layer used for MIM capacitors in MMIC technology. Left: circuit symbol; right: relevant part of the ADS CITIfile used.

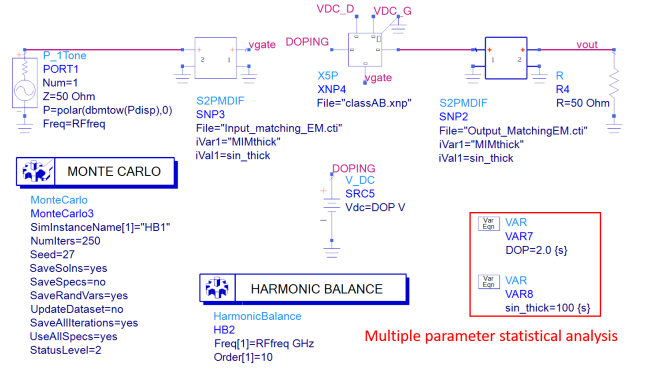


Fig. 4. ADS schematic for statistical analysis with concurrent, fully uncorrelated, variations of the active device (doping) and the passive matching network (SiN layer thickness).

works were limited to the active device variability *per se* [8] or to the PA statistical analysis limited to the output matching network technological variations [1]. The gate port was instead terminated with 50  $\Omega$  and, therefore, highly mismatched. We address here the design of the input matching network, including its statistical variations. Clearly, this can be seen as a source-pull analysis. The X-par model previously extracted with 50  $\Omega$  loads at each port (hereafter referred to as  $X_{50,50}$ ) proved to be accurate for the analysis of the output impedance matching: in fact, for the 1 mm GaAs FET used for the PA design (see [1] for technology details), the optimum power load was  $(43 + j10) \Omega$ , with a real part not far from 50  $\Omega$ . To match the input port, instead, the optimum source impedance needs to be  $2.4 + j20 \Omega$ , significantly different from 50  $\Omega$ . We have therefore extracted a new X-par model with the gate terminated with a resistance of 5  $\Omega$  ( $X_{5,50}$ ), closer to the real part of the optimum source impedance, while keeping 50  $\Omega$  as the load resistance. Load dependent X-par are in fact more prone to model bare devices [10], [11]. To compare

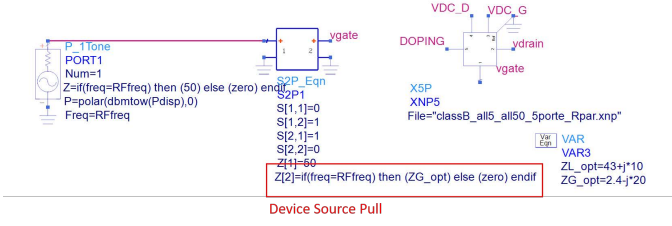


Fig. 5. ADS schematic for source-pull analysis used to validate the X-par model.

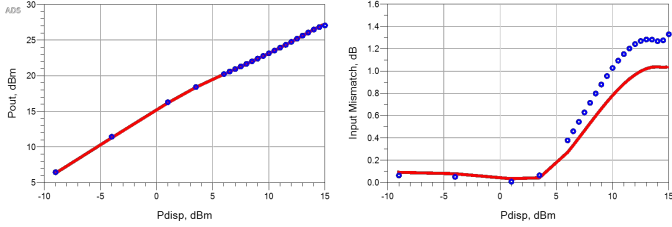


Fig. 6. Output power (left) and input mismatch (right) as a function of the available power. Blue symbols: TCAD simulations. Red solid lines: ADS simulations with the  $X_{50\_50}$

the two models we use the schematic in Fig. 5, where an ideal matching network is used to provide the device with the desired harmonic loads without changing the available source power [12]: notice that this mimics the actual source-pull characterization set-up, where the source impedance is varied by means of tuners. This allows also for a simpler extraction of the X-par from TCAD simulations, where the non linear model is extracted as a function of the generator available power.

Despite  $X_{50\_50}$  is capable to reproduce with good accuracy the device behaviour in terms of the  $P_{in} - P_{out}$  curves and of the input mismatch (see Fig. 6), Fig. 7 shows that the dynamic load lines obtained with  $X_{5\_50}$  follow much better the details of the time-domain waveforms. This becomes important for harmonic loading and variability analysis, since the terminations will not behave as ideal idlers at harmonics. Thus  $X_{5\_50}$  will be used in the following. Interestingly, for the X-par model extraction there is no need to match exactly the optimum source impedance (usually not known *a priori*), but it is sufficient to use a lower value of the gate port resistance, a generally true condition for FETs.

#### IV. POWER AMPLIFIER STATISTICAL ANALYSIS

The optimum source matching impedance has been synthesized first with microstrip transmission lines, and then converted into a semi-lumped circuit, exploiting MIM capacitors to shorten both the stubs and the series lines. The preliminary design is fine tuned to achieve proper loads up to the 5-th harmonic. Finally, the design is converted into the corresponding layout (see Fig. 8) for the final EM simulation through the full-wave planar-3D Momentum simulation engine. For the passive part design and EM simulations we adopted a technology stack-up derived from a

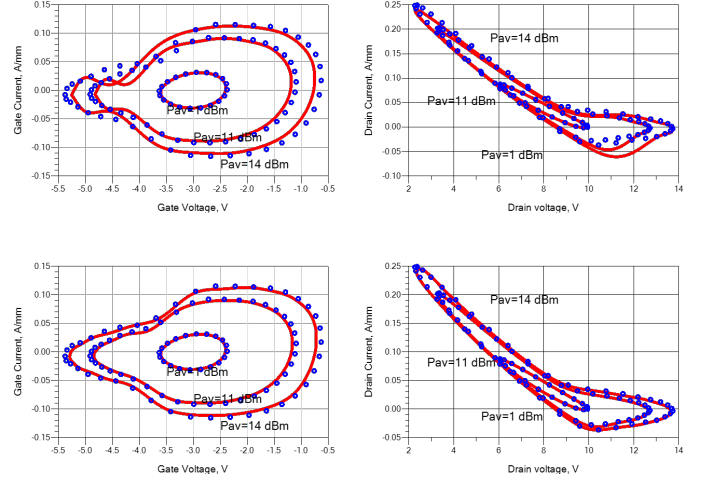


Fig. 7. Comparison of the gate and drain Dynamic Load Lines with  $X_{50\_50}$  (top)  $X_{5\_50}$  (bottom). Blue symbols: TCAD simulations. Red solid lines: ADS simulations.

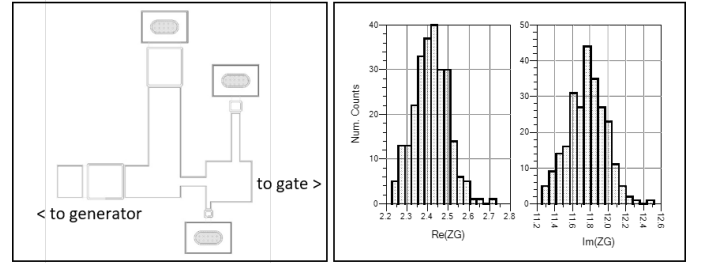


Fig. 8. Layout of input matching network (left) and spread of the impedance presented to the gate with 2% statistical variations of the MIM layer (right).

typical GaAs design kit (DK) suitable for X-band applications, featuring two gold layers (1  $\mu\text{m}$  and 2  $\mu\text{m}$  thick) combined together in micro-strip transmission lines, and a 100 nm-thick SiN insulating layer for MIM capacitors (resulting into about 600 pF/mm<sup>2</sup> capacitance). According to the DK, MIM layer variations are described by a random distribution with standard deviation  $\sigma = 2$  nm around the nominal 100 nm thickness. Therefore, the EM analysis has been carried out with MIM layer values up to  $\pm 3\sigma$ , i.e. uniformly distributed in the interval [94,106] nm. The load termination was designed with the same DK in [1] and has not been changed.

Finally, statistical simulations are performed with uncorrelated variations of the MIM layer thickness (gaussian distribution with  $\sigma = 2$  nm, i.e. 2%) and of the active device doping (also gaussian with  $\sigma = 2\%$  of the nominal value). The thickness of the MIM layer is varied uniformly in the wafer, hence MIM variations in the source and load matching networks are fully correlated. The statistical distribution of the loads resulting from the input matching network is shown in Fig. 8. Fig. 9 shows the spread of the output power obtained by the statistical analysis. To highlight the relative contribution of the two variations, individual doping and MIM variations are first plotted separately. Despite doping variations are

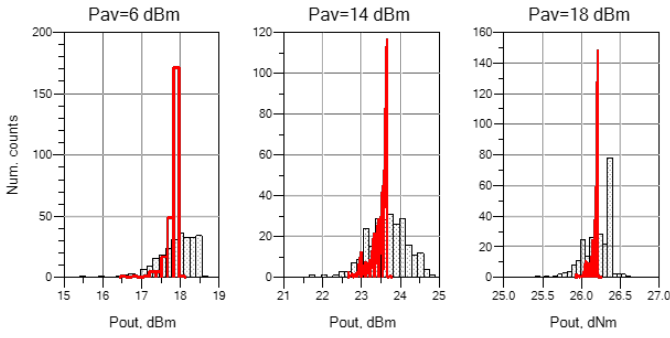


Fig. 9. Output power distribution of the PA stage subject to doping variations (black) and MIM layer variations (red) at different input power levels.

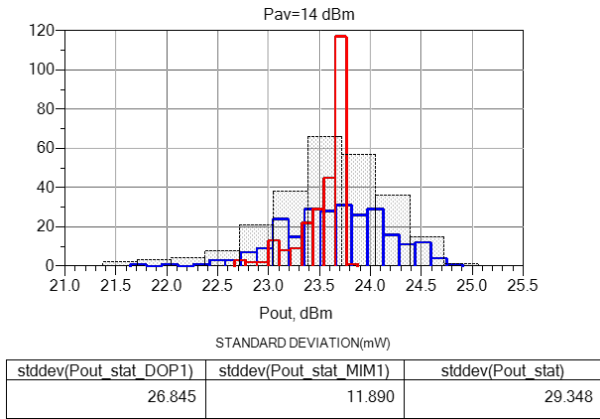


Fig. 10. PA output power distribution subject to separate doping (blue) and MIM layer variations (red) compared to concurrent variations (black).

dominant, MIM variations add significantly to the overall spread. The output power presents a significant skew towards lower power, although the skew amount depends on the input power. The output power spread is highest at intermediate input power, approximately at 5 dB OBO, whereas the spread is minimum at compression. Fig. 10 shows the comparison of the output power variations due to the individual spread along with the concurrent variations. The selected output power corresponds to about 5 dB OBO: in this condition the overall standard deviation is as high as 30 mW over an average of about 230 mW, corresponding to more than 10% uncertainty. With respect to the analysis in [1], where the output matching network was the only variability source, the overall spread has significantly worsened, as shown in Fig. 11: the standard deviation is more than three times higher.

#### ACKNOWLEDGMENT

This work has been supported by the Italian Ministero dell'Istruzione dell'Università e della Ricerca (MIUR) under the PRIN 2017 Project "Empowering GaN-on-SiC and GaN-on-Si technologies for the next challenging millimeter-wave applications (GANAPP)"

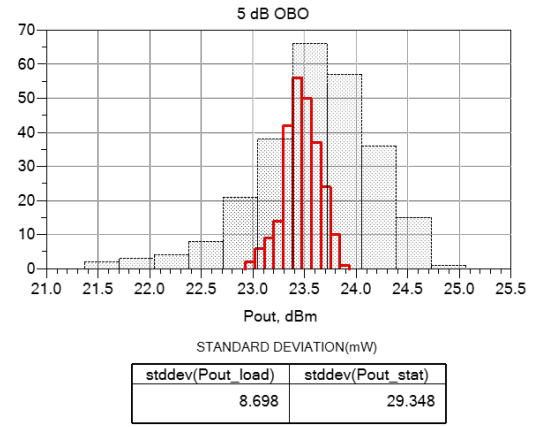


Fig. 11. Output power distribution of the PA stage subject to variations only in the load matching network (red) compared to the spread due to variations in the complete passive networks (black).

#### REFERENCES

- [1] S. Donati Guerrieri, C. Ramella, F. Bonani, G. Ghione, "Efficient sensitivity and variability analysis of nonlinear microwave stages through concurrent TCAD and EM modeling", *IEEE J. on Multiscale and Multiphysics Comp. Techn.*, vol. 4, no. 1, pp. 356–363, 2019.
- [2] <https://www.keysight.com/main/editorial.jsp?cc=US&lc=eng&ckey=1619575&nid=-34346.1255256.08&pid=2952481>
- [3] D. E. Root, J. Verspecht, J. Horn, M. Marcu, *X-parameters*. Cambridge University Press, 2013.
- [4] S. Donati Guerrieri, F. Bonani, F. Bertazzi, G. Ghione, "A Unified Approach to the Sensitivity and Variability Physics-Based Modeling of Semiconductor Devices Operated in Dynamic Conditions - Part I: Large-Signal Sensitivity", *IEEE Trans. Electron Devices*, vol. 63, no. 3, pp. 1195–1201, 2016.
- [5] F. Bertazzi, F. Bonani, S. Donati Guerrieri, G. Ghione, "Physics-based SS and SSLS variability assessment of microwave devices through efficient sensitivity analysis", *Int. Workshop on Integrated Nonlinear Microwave and Millimetre-wave Circuits (INMMIC 2012)*, 3-4 Sept. 2012, Dublin, Ireland.
- [6] S. Donati Guerrieri, F. Bonani, M. Pirola, "Concurrent Efficient Evaluation of Small-Change Parameters and Green's Functions for TCAD Device Noise and Variability Analysis", *IEEE Trans. El. Dev.*, Vol. ED-64, No: 3, pp.1269–1275, Feb. 2017.
- [7] S. Donati Guerrieri, F. Bonani, G. Ghione, "Linking X Parameters to Physical Simulations For Design-Oriented Large-Signal Device Variability Modeling", *Int. Microw. Symp. (IMS 2019)*, Boston (MA), 2019.
- [8] S. Donati Guerrieri, F. Bonani, G. Ghione, "A comprehensive technique for the assessment of microwave circuit design variability through physical simulations", *Int. Microw. Symp. (IMS 2017)*, 4-9 June 2017, Honolulu, HI, USA.
- [9] S. Donati Guerrieri, F. Bonani, G. Ghione, "Physically-based statistical analysis of nonlinear circuits through X-parameters", *14th European Microwave Integrated Circuits Conference (EuMIC 2019)*, 30 Sept.-1 Oct. 2019, Paris, France.
- [10] R. M. Biernacki, M. Marcu, D. E. Root, "Circuit Optimization with X-Parameter Models", *Int. Microw. Symp. (IMS 2017)*, Honolulu (HW), 2017.
- [11] H.-F. Hsiao, C.-H. Tu, D.-C. Chang, "Non-fifty Ohm X-parameter Model Measurement System for Nonlinear Amplifier Application", *2018 IEEE International Instrumentation and Measurement Technology Conference (I2MTC)*, 14-17 May 2018, Houston, TX, USA.
- [12] [https://www.keysight.com/upload/cmc\\_upload/All/EuMW2011\\_XparPADesign.pdf](https://www.keysight.com/upload/cmc_upload/All/EuMW2011_XparPADesign.pdf)